https://doi.org/10.5194/acp-2021-228
Preprint. Discussion started: 22 April 2021

Atmospheric Chemistry and Physics Discussions

Reactions of NO_3 with Aromatic Aldehydes: Gas Phase Kinetics and Insights into the Mechanism of the Reaction

Yangang Ren,[1] Li Zhou,[1,2] Abdelwahid Mellouki,[1,3 *] Véronique Daële,[1] Mahmoud Idir,[1] Steven S. Brown,[4,5] Branko Ruscic,[6] Robert S. Paton,[7] Max McGillen,[1] and Akkihebbal R. Ravishankara[1,7,8,9 *]

1. Institut de Combustion Aérothermique, Réactivité et Environnement, Centre National de la Recherche Scientifique (ICARE-CNRS), Observatoire des Sciences de l'Univers en région Centre (OSUC), CS 50060, 45071 cedex02 Orléans, France
2. Present address: College of Architecture and Environment, Sichuan University, Chengdu, 610065, China.
3. Environment Research Institute, School of Environmental Science and Engineering, Shandong University, Qingdao 266237, China
4. NOAA, Chemical Sciences Laboratory, Boulder, CO USA
5. Department of Chemistry, University of Colorado, Boulder, CO USA
6. Chemical Sciences and Engineering Division, Argonne National Laboratory, Lemont, IL 60439, USA
7. Department of Chemistry, Colorado State University, Fort Collins, CO USA
8. Department of Atmospheric Science, Colorado State University, Fort Collins, CO USA
9. Le Studium Institute for Advanced Studies, Orléans, France

*: Address correspondence to:
mellouki@cnrs-orleans.fr or A.R.Ravishankara@Colostate.edu.

https://doi.org/10.5194/acp-2021-228
Preprint. Discussion started: 22 April 2021

Atmospheric Chemistry and Physics Discussions

Abstract: Rate coefficients for the reaction of NO_3 radicals with a series of aromatic aldehydes were measured in a 7300 liter simulation chamber at ambient temperature and pressure by relative and absolute methods. The rate coefficients for benzaldehyde (BA), ortho-tolualdehyde (O-TA), meta-tolualdehyde (M-TA), para-tolualdehyde (P-TA), 2,4-dimethyl benzaldehyde (2,4-DMBA), 2,5-dimethyl benzaldehyde (2,5-DMBA) and 3,5-dimethyl benzaldehyde (3,5-DMBA) were: k_1 = 2.6 ± 0.3, k_2 =8.8 ± 0.8, k_3 = 4.8 ± 0.5, k_4 = 4.9 ± 0.5, k_5 = 15.1 ± 1.4, k_6 = 12.7 ±1.2 and k_7 = 6.2 ±0.6, respectively, in the units of 10^{-15} cm^3 $molecule^{-1}$ s^{-1} at 298±2 K. The rate coefficient k_{13} for the reaction of the NO_3 radical with deuterated benzaldehyde (benzaldehyde-d_1) was found to be half that of k_1. The end product of the reaction with an excess of NOx was measured to be $C_6H_5C(O)O_2NO_2$. Theoretical calculations of aldehydic bond energies and reaction pathways indicate that NO_3 radical reacts with aromatic aldehydes through the abstraction of aldehydic hydrogen atom. The atmospheric implications of the measured rate coefficients are briefly discussed.

Keywords: rate coefficient, NO_3 radical, aromatic aldehydes, mechanism

https://doi.org/10.5194/acp-2021-228
Preprint. Discussion started: 22 April 2021

Atmospheric Chemistry and Physics Discussions

1. Introduction

Aromatic aldehydes are a family of organic compounds emitted into the atmosphere from anthropogenic and biogenic sources. For example, benzaldehyde (BA) has been detected in the incomplete combustion of fuels (Legreid et al., 2007). Methylated benzaldehydes (ortho, meta, para-tolualdehydes) are present in wood smoke and biomass burning plumes (Koss et al., 2018). Benzaldehyde also has extensive industrial usage in perfume, soap, food and drink production, and as solvent for oils and resins (OECD, 2002). BA and ortho/meta/para-tolualdehyde could also be formed from the atmospheric degradation of aromatic hydrocarbons, although their yields in the atmosphere are expected to be small (Calvert et al., 2002;Obermeyer et al., 2009).

It is believed that their reaction with the OH radical dominates the photochemical loss of aromatic aldehydes. Yet, oxidation of aromatic aldehydes via their reaction with the nitrate radical, NO_3, may be important in NOx-rich locations at night since both the aromatic aldehydes and the nitrate radical can arise from anthropogenic emissions and biomass burning. Therefore, aromatic aldehydes can be degraded at night with consequences for ozone and secondary organic aerosol (SOA) formation. The reactions of aromatic aldehydes with NO_3 likely leads to acyl peroxy nitrates (APNs, often also referred to as PANs) in the NOx-rich regions with characteristically high NO_3 abundances. The APNs would then transport nitrogen oxides and the aromatic moieties from the polluted to cleaner parts of the globe (Wayne, 2000) with consequences for ozone production and particle formation away from the polluted regions. Therefore, quantifying the kinetics and understanding the mechanism of the reaction of NO_3 with aromatic aldehydes is needed.

In this study, the rate coefficients k_1-k_7 at 298 K for the reactions of NO_3 radical with the following seven aromatic aldehydes were measured:

benzaldehyde (BA) + NO_3 → products; k_1 (1)

ortho - Tolualdehyde (O-TA) + NO_3 → products; k_2 (2)

meta - Tolualdehyde (M-TA) + NO_3 → products; k_3 (3)

para - Tolualdehyde (P-TA) + NO_3 → products; k_4 (4)

2,4 - dimethyl benzaldehyde (2,4-DMBA) + NO_3 → products; k_5 (5)

2,5 - dimethyl benzaldehyde (2,5-DMBA) + NO_3 → products ; k_6 (6)

3,5 - dimethyl benzaldehyde (3,5-DMBA) + NO_3 → products; k_7 (7)

The rate coefficient for Reaction (1) has been previously reported by Carter et al.,(1981), Atkinson et al.,(1991), Clifford et al.,(2005) and Bossmeyer et al.,(2006) The rate coefficients for Reactions 2-4 were reported only by Clifford et al.,(2005). There are no previous reports on k_5-k_7, to the best of our knowledge. The results from earlier studies are compared with our data in a later section.

https://doi.org/10.5194/acp-2021-228
Preprint. Discussion started: 22 April 2021

Atmospheric Chemistry and Physics Discussions

We report the rate coefficients at 298 K for the above reactions and we have determined the stable products formed in Reaction (1). We also have attempted to elucidate the mechanism of these reactions via studies of isotopic substitution, quantum chemistry calculations, and an examination of the linear free energy relationship.

2. Experimental setup and procedures

The kinetics and products were studied in a 7300 liter indoor simulation chamber described in detail previously (Zhou et al., 2017); therefore, it is described only briefly here. The chamber was made of Teflon foil. Two Teflon fans located inside the chamber rapidly mixed the contents of the chamber within about 30 s. Purified air was used as a bath gas and to flush the chamber to clean it in between experiments. Upon flushing, the levels of NO_2 and O_3 were less than 50 pptv (detection limit of our instruments). A proton transfer reaction time-of-flight mass spectrometer (PTR-TOF-MS) and a Fourier transform infrared spectrometer (FT-IR, Nicolet 5700) coupled to a White-type multipass cell (143 m optical path length) were employed to monitor the organic compounds in the chamber. The white cell was located within the chamber. An inlet situated in the center of the chamber fed the PTR-TOF-MS. The masses in PTR-TOF-MS and IR lines in the FTIR were used to measure the aldehydes that are listed in the SI (Table S1). The PTR-TOF-MS and/or FTIR signals were measured as a function of manometrically determined hydrocarbons concentrations. Calibration plots for the quantification of the aromatic aldehydes and the reference gases were constructed using these measurements. They are shown in Figure S1 in the SI. The concentrations of NO_3 and N_2O_5 were determined using a cavity ring down spectrometer (CRDS). The NO_3 radical was detected using its strong 662 nm absorption. The sum of NO_3 and N_2O_5 were detected simultaneously by thermally dissociating N_2O_5 in a second channel. The time resolution of CRDS was 1s, and detection limits for NO_3 and N_2O_5 were approximately 0.5 pptv for a 5 s intergration (Brown et al., 2002;Dubé et al., 2006). NO_3 radicals were generated from the thermal decomposition of N_2O_5 in the chamber.

2.1 Rate coefficient measurements

Relative Method: The temporal profiles of a reference compound and the aromatic aldehyde of interest were monitored simultaneously using the PTR-TOF-MS and/or FTIR in the presence of NO_3 radical.

NO_3 + aromatic aldehydes → products ; $k_{1\text{-}7}$

NO_3 + references → products ; k_{ref}

https://doi.org/10.5194/acp-2021-228
Preprint. Discussion started: 22 April 2021

Atmospheric Chemistry and Physics Discussions

We accounted for the dilution of the chamber necessitated by the addition of air to keep the pressure constant while we continually withdrew the chamber's contents for analysis. Similarly, we also accounted for the depletion of the hydrocarbons due to the loss to the walls. The two processes together are represented as a first order loss process with a rate coefficient k_d:

aromatic aldehydes/references → wall loss/dilution ; k_d

Above, $k_{1\text{-}7}$ and k_{ref} are the rate coefficient for the reaction of NO_3 with studied aromatic aldehydes (BA, O-TA, M-TA, P-TA, 2,4-DMBA, 2,5-DMBA, and 3,5-DMBA) and the reference compound (methyl methacrylate, MMA), respectively. The dilution rate coefficient was measured by adding a small amount of unreactive SF_6 into the chamber and watching its temporal decay. We quantified the rate coefficient (ranging from 5.5×10^{-7} s^{-1} to 1.6×10^{-6} s^{-1}) for the removal of the aldehydes and reference compound due to loss on the walls by monitoring their decay in the absence of the NO_3 reactant

The typical experimental procedure for relative rate measurements consisted of a sequence of three steps: (1) SF_6 was added and monitored for about 30 mins to measure the dilution rate coefficient; (2) VOCs (aromatic aldehydes, reference compounds) were introduced into the chamber and monitored for roughly 30 minutes to obtain k_d; and (3) N_2O_5 was then continually introduced to the chamber using pure air as a carrier gas, and the consumption of VOCs was monitored using PTR-TOF-MS for 1-2 hours. The typical initial VOC concentrations were (0.9-4.5) $\times$ 10^{12} molecule cm^{-3} (Table S2). Typical NO_3 concentrations were (0.25-2.5) $\times$ 10^9 molecule cm^{-3}.

Assuming that the aromatic aldehydes and reference compounds were lost by reaction with NO_3 radical and dilution/loss to the walls, it can be shown that:

$$\ln\left(\frac{[aro]_0}{[aro]_t}\right) - k_d \times t = \left(\frac{k_{1-7\_RR}}{k_{ref}}\right) \times \left[\ln\left(\frac{[ref]_0}{[ref]_t}\right) - k_d \times t\right] \qquad \text{I}$$

Where $[aro]_0$ and $[aro]_t$, and $[reference]_t$ and $[reference]_0$, are the corresponding concentrations of aromatic aldehydes and reference compound at initial time and time t, respectively. According to Equation I, plots of $\{\ln\left(\frac{[aro]_0}{[aro]_t}\right) - k_d \times t\}$ against $\{\ln\left(\frac{[ref]_0}{[ref]_t}\right) - k_d \times t\}$ are straight lines of slope equal to $k_{1\text{-}7}/k_{ref}$, with zero intercepts.

Absolute method: Experiments were conducted in the same 7300 liter simulation chamber described in the previous section. The temporal profiles of NO_3 and N_2O_5 were measured using

https://doi.org/10.5194/acp-2021-228
Preprint. Discussion started: 22 April 2021


Atmospheric Chemistry and Physics Discussions

CRDS in an excess of each aromatic aldehyde (Zhou et al., 2017), and were simultaneously fit to a reaction scheme (see below) to extract the reaction rate coefficient as described by Zhou et al., (2017). The typical experimental procedure consisted of the following steps: (1) N_2O_5 was introduced with pure air into the chamber and the temporal profiles of NO_3 and N_2O_5 concentrations were measured to determine the rate coefficient for loss of NO_3 and N_2O_5 to the walls, reactions with impurities, and dilution; (2) The aromatic aldehyde of interest was introduced while continually measuring the temporal profiles of NO_3 and N_2O_5; and (3) SF_6 was introduced to determine the dilution rate when needed.

To obtain the rate coefficients of NO_3 radical reaction with aromatic aldehydes, a box model was used to integrate the set of Reactions (1-11), and the obtained temporal profiles of NO_3 and N_2O_5 concentrations were fit to the observed profiles using a non-linear least squares algorithm.

$$NO_3 + NO_2 \rightarrow N_2O_5 \; ; \; k_8 \qquad (8)$$

$$N_2O_5 \rightarrow NO_3 + NO_2 \; ; \; k_9 \qquad (9)$$

$$NO_3 \rightarrow \text{wall loss} \; ; \; k_{10} \qquad (10)$$

$$N_2O_5 \rightarrow \text{wall loss} \; ; \; k_{11} \qquad (11)$$

$$NO_3 + \text{aromatic aldehydes} \rightarrow \text{products} \; ; \; k_{1\text{-}7} \qquad (1\text{-}7)$$

In the algorithm, the sum of squares of both the NO_3 and N_2O_5 were minimized while varying the input parameters. In the absence of the aldehydes, the input parameter was just k_d. The value of k_d obtained was then held constant when subsequently fitting the second set of temporal profiles where the rate coefficient for reactions (1)-(7) were varied. The other input parameters included the measured initial concentration of NO_3 ($[NO_3]_0$), N_2O_5 ($[N_2O_5]_0$), and the initial aromatic aldehydes ($[aro]_0$) as well as the temperature dependent values of k_8 and k_9 (to define the equilibrium constant (k_{eq})). The equilibrium constant for the reaction: $NO_3 + NO_2 \rightleftharpoons N_2O_5$ by Burkholder et al.,(2015) was used. The NO_2 concentration was calculated through the equilibrium constant and measured concentrations of NO_3 and N_2O_5 throughout the course of the reactions; i.e., $[NO_2]=[N_2O_5]/([NO_3]\times k_{eq})$ and used in the fits. Such calculated temporal profiles of NO_3 and N_2O_5 were fit to the measured temporal profiles at various concentrations of the aldehydes. As shown in Table S3, the concentration of aromatic aldehyde was always 50-1500 times higher than that of NO_3 in the chamber at all times, and thus NO_3 loss was essentially first order in its concentration.

2.2 Chemicals

The aromatic aldehydes were purchased from Sigma-Aldrich. The stated purities of these chemicals were: benzaldehyde (≥ 99.5%), O-TA (97%), M-TA (97%), P-TA (≥ 97%), 2,4-

https://doi.org/10.5194/acp-2021-228
Preprint. Discussion started: 22 April 2021

Atmospheric Chemistry and Physics Discussions

DMBA (≥ 90%), 2,5-DMBA (99%) and 3,5-DMBA (97%). Methyl methacrylate was bought from TCI. The chemical purity of benzaldehyde-α-d1 was 99% while its isotopic purity was 98%. All the aldehydes (in liquid form) were further purified by repeated freeze-pump-thaw cycles before use. Substantial concentrations of reactive impurities were not detected in these samples based on the PTR-TOF-MS/FTIR measurements. A mixture of NO_2 and O_3 was flowed into a 1 liter bulb to generate N_2O_5 through Reactions 12 and 8.

$$NO_2 + O_3 \rightarrow NO_3 + O_2 \; ; k_{12} \quad (12)$$

$$NO_3 + NO_2 \rightarrow N_2O_5 \; ; k_8 \quad (8)$$

The N_2O_5 crystals were collected in a cold trap (190 K) and purified by trap-to-trap distillation in a mixture of O_2/O_3. N_2O_5 was stored in a cold trap maintained 190 K.

3. Results and Discussion

3.1 Rate coefficients determination of NO_3 reaction with a series of aromatic aldehydes

In the study, we measured the rates coefficients k_1-k_7 using a relative method and an absolute method. They are outlined separately below for ease of presentation.

3.1.1 Relative method

Methyl methacrylate, MMA, was used as the reference compound in this work because the rate coefficient at 298 K for its reaction with NO_3 radical is well established (Zhou et al., 2017) to be $k_{MMA}=(2.98\pm0.35)\times10^{-15}$ cm^3 $molecule^{-1}$ s^{-1}. The experimental conditions and associated parameters are shown in Table S2.

Figure 1 shows plots of $\{\ln(\frac{[aro]_0}{[aro]_t}) - k_d \times t\}$ against $\{\ln(\frac{[ref]_0}{[ref]_t}) - k_d \times t\}$ for the seven aromatic aldehydes. Each plot is linear with an intercept of zero within the uncertainties. The $k_d \times t$ term is relatively small (3.6-7.6%) compared to the ratio $\{\frac{k_d \times t}{\ln(\frac{[aro]_0}{[aro]_t}) \text{ or } \ln(\frac{[ref]_0}{[ref]_t})}\}$, and small variations in its value do not affect the accuracy of the measured rate coefficients. Figure 1 also shows that the measured values of the rate coefficient ratios are reproducible. The ratios of rate coefficients, $\frac{k_{1,7}}{k_{ref}}$, were calculated from these plots using the algorithm of Brauers and Finlayson-Pitts (1997), which takes into account errors in both the abscissa and ordinate. These errors were estimated from the uncertainty of the concentration calculated from the calibration plots generated before the kinetics runs. The noted errors for $\frac{k_{1,7}}{k_{ref}}$ are twice the standard deviation in the least-squares fits multiplied by a factor to account for the limited number of measurements using the Student *t*-distribution.

https://doi.org/10.5194/acp-2021-228
Preprint. Discussion started: 22 April 2021

Atmospheric Chemistry and Physics Discussions

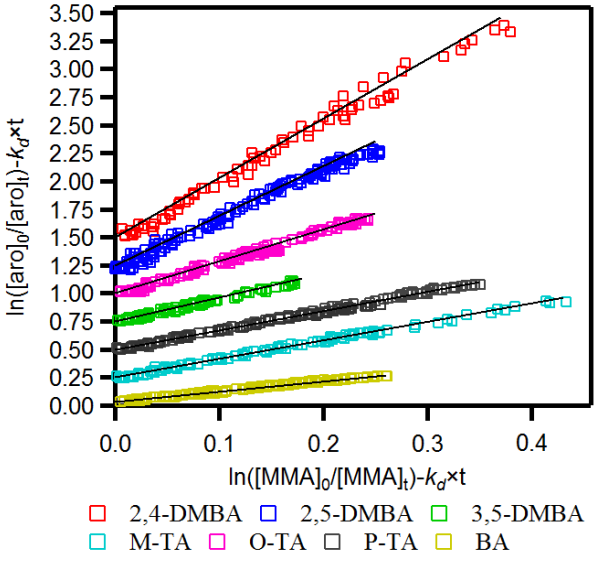

Figure 1. Plots of relative kinetic data obtained from the reaction of aromatic aldehydes (aro) with NO_3 radical using methyl methacrylate (MMA) as the reference. M-TA, P-TA, 3,5-DMBA, O-TA, 2,5-DMBA and 2,4-DMBA were shifted 0.25, 0.5, 0.75, 1.0, 1.25, and 1.5, respectively, for clarity.

The relative rate coefficients of the studied aromatic aldehydes, termed k_{RR}, are shown in Table S2. The estimated uncertainties for k_{RR} were the sum of the precision of our measurements (noted above) and the quoted uncertainties in the rate coefficient for the reference reaction according to the expression:

$$\sigma(k_{RR}) = \frac{k}{k_{ref}} \times k_{ref} \sqrt{\left[\frac{\sigma k_{ref}}{k_{ref}}\right]^2 + \left[\frac{error}{\frac{k}{k_{ref}}}\right]^2}.$$

3.1.2 Absolute method

The method used to analyze the temporal profiles of NO_3 and N_2O_5 to obtain k_1-k_7 has been described by Zhou et al. (2017;2019). Figure 2 shows an example of the temporal profiles of NO_3 and N_2O_5 for Reaction (1) from which the rate coefficient k_1 was derived. Similar analyses yielded k_2-k_7 (Figure S2-7).

Panel (a) of Figure 2 shows the temporal profile of NO_3 and N_2O_5 concentrations plotted on a logarithmic scale. The concentrations decrease exponentially (the lines are linear), and the decay rates are lower in the absence of the reactant aldehyde than in its presence. The rate coefficients for the loss of NO_3 and N_2O_5 to the walls and dilution, k_{10} and k_{11}, were determined

https://doi.org/10.5194/acp-2021-228
Preprint. Discussion started: 22 April 2021


Atmospheric Chemistry and Physics Discussions

to be in the ranges (3.7-7.1)×10^{-3} s^{-1} and (3.2-12.0)×10^{-4} s^{-1}, respectively. As explained in Zhou et al.,(2017), we cannot merely take the slopes of decay of NO_3 with time to calculate the rate coefficients k_1-k_7 since NO_3 and N_2O_5 are coupled through their equilibrium. The equilibration is maintained throughout the course of Reactions (1)-(7). To account for this situation, we fit the profiles of both NO_3 and N_2O_5 to a reaction scheme, as described previously.

Panels (b) and (c) of Figure 2 show the NO_3 and N_2O_5 temporal profiles on a linear scale in the absence and in the presence of the reactant aldehyde. The two panels also show the fits of the data to the mechanism that included only Reactions (1)-(11). The fits are acceptable but with larger variations at longer reaction times. We have to consider the contributions to NO_3 and N_2O_5 losses due to the reactions of NO_3 with the products of the Reactions (1)-(7). Values of the rate coefficients derived from such fits included all the potential reactions that can contribute to the removal of NO_3, and they are shown in the SI (Table S4). When the secondary reactions with the products were included, the fits were better at the longer reaction times, and they are shown in Panel (d) of Figure 2. The residuals of the fits are shown at the bottoms of panel (c) and (d); they clearly show the improvement in the fits and the lack of a trend with reaction time. Larger deviations are to be expected in panel (c) at longer reaction times as the products of the reactions build up. The rate coefficients k_1-k_7 calculated using the reaction scheme shown in Table S4 are taken to be those measured by the direct method. As expected, the rate coefficients calculated by including the contributions of the secondary reactions were slightly less than those without the secondary reaction contributions (see Figure S8). The differences were on the average about 5%.

https://doi.org/10.5194/acp-2021-228
Preprint. Discussion started: 22 April 2021

Atmospheric Chemistry and Physics Discussions

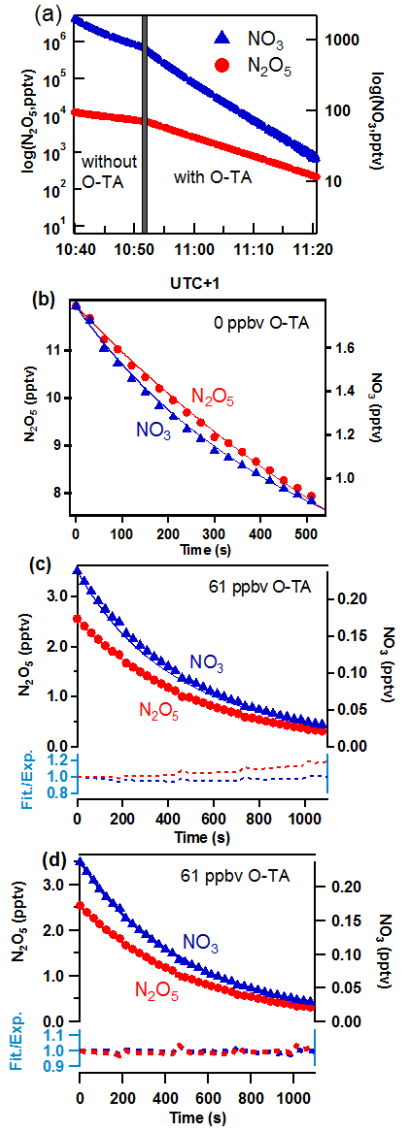

Figure 2 Observed (points) and simulated (lines) profiles of N_2O_5 (left axis) and NO_3 (right axis) as a function of time. Mixing ratios of o-tolualdehyde are shown in each panel. Panel (a): the time profiles on a log scale. Panel (b): Temporal profiles in linear scale and the fits to the data as discussed in the text. Panel (c): Fits of simulations not including the subsequent secondary reactions of NO_3 with the products of the initial reaction. The dash lines at the bottom show the ratio of simulated lines to measured data points (Fit./Exp.) for NO_3 (blue) and N_2O_5 (red). Panel (d): Fits of simulations including the subsequent secondary reactions of NO_3 with the initial reaction products (shown in Table S4). The dash lines at the bottom show the ratio of

https://doi.org/10.5194/acp-2021-228
Preprint. Discussion started: 22 April 2021


Atmospheric Chemistry and Physics Discussions

simulated lines to measured data points (Fit./Exp.) for NO_3 (blue) and N_2O_5 (red). The improvements in the fits are clear in Panel (d).

The results of our measured values for $k_{1\text{-}7}$ are summarized in Table S3. The quoted errors of the rate coefficient from each experiment are at the 95% confidence level based on the precision of the fits; they were typically less than 7%. The weighted averages of results from multiple experiments were calculated, and then the influence of the small number of measurements were accounted for by using a Student *t*-distribution table. We added the estimated systematic uncertainties to the precision in quadrature, assuming that they are uncorrelated. Contributions to estimated systematic errors included: (1) The systematic errors of -8/+11% and -9/+12%, respectively, in the measurements of NO_3 and N_2O_5 (Zhou et al., 2019); (2) The uncertainty of around 10% in the rate coefficients used in the reaction schemes shown in Table S4; and (3) The estimated uncertainty of 7% in the concentration of aromatic aldehydes. This includes the uncertainties in the calibration and spectral analysis. All the noted uncertainties are at the 95% confidence level, assuming a Gaussian error distribution.

It is important to note that we need the absolute concentrations of NO_3 and N_2O_5 even though the reaction was first order in NO_3 due to the strong coupling between the concentrations of NO_3 and N_2O_5 via an equilibrium. The presence of the aldehydes would influence the temporal profiles of both N_2O_5 and NO_3. Here we are attributing the entire change to the reaction of NO_3 with the aldehydes. The validity of this assumption is shown by the measured rate coefficients being independent of the ratio of $[NO_3]/[N_2O_5]$. This ratio was changed simply by changing $[NO_2]$ that shifts the equilibrium concentrations of NO_3 and N_2O_5.

3.1.3 Comparison of Rate coefficients obtained from absolute and relative methods

The rate coefficients for the reactions of NO_3 with 7 different aromatic aldehydes, k_1-k_7, measured using the absolute and relative methods are summarized in Table 1. The rate coefficient values from the two methods are in good agreement with each other. The differences are less than 10%, except for k_1, which differs by 18%. They, however, overlap within the combined errors of our measurements.

As shown in Table S5, the final rate coefficients of 7 aromatic aldehydes reaction with NO_3 radical were derived from the weighted average of the absolute and the relative rate methods, using the equation discussed above (Eq. S2 and Eq. S3).

https://doi.org/10.5194/acp-2021-228
Preprint. Discussion started: 22 April 2021

Atmospheric Chemistry and Physics Discussions

Table 1. Rate constants k_1-k_7 measured in the study using two different methods.

Aromatic aldehydes	rate constants (10^{-15} cm^3 molecule^{-1} s^{-1})		ratio	k_{final}[a]
	k_{RR}	k_{AR}	(k_{RR}/k_{AR})	(10^{-15} cm^3 molecule^{-1} s^{-1})
BA	2.8±0.4	2.3±0.4	1.18	2.5±0.3
O-TA	8.5±1.1	9.1±1.2	0.94	8.8±0.8
M-TA	5.0±0.7	4.7±0.6	1.05	4.8±0.5
P-TA	5.1±0.7	4.8±0.6	1.06	4.9±0.5
2,4-DMBA	15.8±2.1	14.6±2.0	1.08	15.1±1.4
2,5-DMBA	13.2±1.7	12.2±1.7	1.08	12.7±1.2
3,5-DMBA	6.3±0.8	6.1±0.8	1.04	6.2±0.6

[a] weighted average values and their error were calculated using Eq.S2 and Eq.S3

3.1.4 Comparison with the literature for NO_3 radical kinetic with aromatic aldehydes

Table S5 summarizes the rate coefficients measured in this work with data from the literature for the reactions of the NO_3 radical with aromatic aldehyde, BA, O-TA, M-TA, P-TA, 2,4-DMBA, 2,5-DMBA, and 3,5-DMBA. As shown in Table S5, the rate coefficient for BA has been reported by five studies. Three of them (Atkinson et al., 1984;Carter et al., 1981;Clifford et al., 2005) used the relative method with different reference compounds. Atkinson et al.,(1991) corrected the values from their earlier report, and they are used for the comparison. Bossmeyer et al.,(2006) measured both NO_3 and BA using differential optical absorption spectroscopy (DOAS) in their chamber. They measured the loss of BA in a known (measured continuously) NO_3 concentration and fitted BA's measured temporal profile to obtain k_1. Calvert et al.,(2011) recommended k_7 to be 4.0 $\times 10^{-15}$ cm^3 molecule^{-1} s^{-1} with a 30% uncertainty based on these studies. However, our value from absolute and relative methods using methyl methacrylate as reference (its rate coefficient has been determined using absolute method in our previous study (Zhou et al., 2017) are in good agreement with Atkinson (1991) and Bossmeyer et al., (2006). Hence, we suggest that the weighted average based on these three studies, 2.6±0.3 $\times 10^{-15}$ cm^3 molecule^{-1} s^{-1} at 298±2 K, is a reliable value. The rate coefficients for ortho/meta/para-tolualdehyde have only been studied by Clifford et al.,(2005) who reported them to be (9.8±0.4), (9.5±0.4) and (9.5±0.7) $\times 10^{-15}$ cm^3 molecule^{-1} s^{-1}, respectively. In this work, k_1-k_7 were determined by relative (MMA as the reference) and absolute methods to be: (8.5±1.1 & 9.1±1.2), (5.0±0.7 & 4.7±0.6) and (5.1±0.7 & 4.8±0.6) $\times 10^{-15}$ cm^3 molecule^{-1} s^{-1}, respectively. This work agrees best with the value of Clifford *et al.*,(2005) for ortho-tolualdehyde, but those of k_3 and k_4 are smaller than those of Clifford et al.,(2005). The reasons for these discrepancies are unclear, but the excellent agreement (<7% difference) between the two techniques presented here give us confidence in our determinations. This work provides the first experimental determinations of the rate coefficients for NO_3 reactions with 2,4-DMBA, 2,5-DMBA, and 3,5-DMBA, where the two complementary methods agree well. The recommended rate coefficients of the weighted average of relative method and absolute method are shown in Table S5.

https://doi.org/10.5194/acp-2021-228
Preprint. Discussion started: 22 April 2021

Atmospheric Chemistry and Physics Discussions

3.2 Mechanisms of the reactions

3.2.1 Products investigation from the reaction of benzaldehyde with NO_3

The stable products formed in Reaction (1) were investigated at 298±2 K and 760 torr in the same 7300 liter simulation chamber. Benzaldehyde, 0.9-1.4×10^{13} molecule cm^{-3} (as shown in Table S6) was introduced into the chamber and its removal was measured for 2 hours to obtain the wall loss rate coefficient. Then, roughly 1.1×10^{12}-1.5×10^{14} molecule cm^{-3} of N_2O_5 was introduced. Stable products formed in the chamber were identified and quantified (when possible) using the PTR-TOF-MS and FTIR.

Two stable products, $C_6H_5C(O)O_2NO_2$ (benzaldehyde-PAN; BAPAN) and $C_6H_5ONO_2$, were detected and measured. The former was detected using both PTR-TOF-MS (m/z 184.024 and its fragment m/z 105.034) and FTIR (965-1005 cm^{-1} centered at 989 cm^{-1}) and the latter using only PTR-TOF-MS. Since we do not have a sample of BAPAN, we could not quantify the yield of this product using PTR-TOF-MS. However, Caralp *et al.*,(1999) have reported the IR band strengths for BAPAN. Using their reported band strength, we could quantify BAPAN to be 80±10% of the benzaldehyde that was removed via reaction, where the quoted uncertainty is the precision in the fit at the 2 σ level. When we account for the uncertainties in the absorption cross sections of BAPAN reported by Caralp et al., (1999) (~20%) and the uncertainties in the concentration of initial benzaldehyde concentration (~10%), and add the precision of the measurements, we conclude that the yield of BAPAN is 80±22%. We assume that the uncertainties are uncorrelated and hence added them in quadrature. The obtained BAPAN amounts are shown in Figure 3 as the function of benzaldehyde consumption; the details are shown in Table S6 in the SI. We could not quantify $C_6H_5ONO_2$ because of the lack of a standard. Assuming that the ion-molecule reaction rate coefficients for proton transfer to BAPAN and $C_6H_5ONO_2$ are similar, we estimate that the yield of $C_6H_5ONO_2$ is smaller than that of BAPAN. These two products are expected if the reaction proceeds via H atom abstraction, most of the peroxy radical reacts with NO_2 (Platz et al., 1998) as denoted by the reaction scheme A:

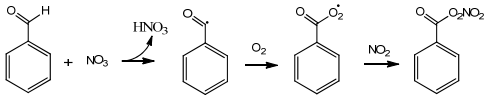

(A)

A fraction of the peroxy radicals react with itself (or other peroxy radicals) to make the phenoxy radical, which ultimately leads to a nitrate, according to the mechanism B:

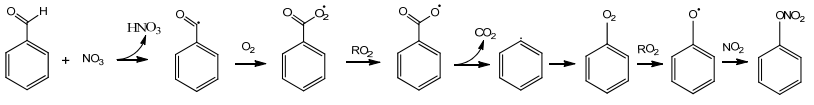

(B)

https://doi.org/10.5194/acp-2021-228
Preprint. Discussion started: 22 April 2021

Atmospheric Chemistry and Physics Discussions

Unfortunately, we could not reduce the concentration of NO_2 sufficiently to completely suppress pathway B. A small fraction of the $C_6H_5C(O)O_2$ would also react with NO_3 but would still yield the $C_6H_5C(O)O$ radicals. Also, any reactions of phenyl radical with NO_2 can be neglected because of the large abundance of O_2 that will quickly convert it to $C_6H_5O_2$ radical. Numerical modeling of the reaction sequence shown in the SI (Table S4) suggests that the yield of BAPAN is more than 95% under our experimental conditions. Based on these results, we suggest the yield of BAPAN in our reaction system is essentially 1 and that we detect the nitrate because of the excellent sensitivity for its detection in our PTR-TOF-MS.

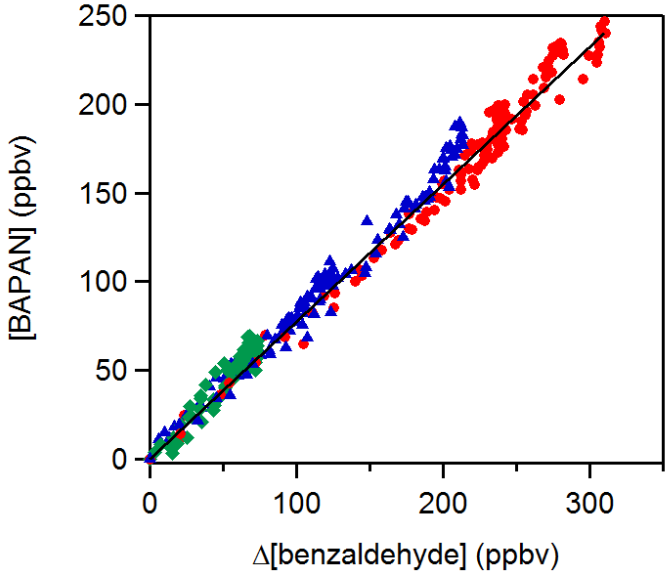

Figure 3. A plot of benzaldehyde PAN ($C_6H_5C(O)O_2NO_2$; BAPAN) concentrations measured by FTIR as a function of depletion of benzaldehyde. The slope of the plot gives the yield of the BAPAN in the NOx-rich environment to be roughly 80±20%.

3.2.1 Kinetic Isotope Effect in the reaction

To further examine the mechanism of NO_3 reactions with the aromatic aldehydes, we measured the rate coefficient for the reaction of NO_3 radical with benzaldehyde-α-d1 (C_6H_5CDO):

$$C_6H_5C(O)D + NO_3 \rightarrow \text{products} ; k_{13} \quad (13)$$

As shown in Figure 4, k_{13} is half that of k_1, i.e., k_1/k_{13} is 1.92. A factor of 2 decrease in the rate coefficient going from benzaldehyde to benzaldehyde-α-d1 is consistent with a primary kinetic isotope effect (KIE), suggesting that abstraction of the aldehydic H atom occurs in the rate-limiting step of this reaction pathway (See calculated KIE below).

https://doi.org/10.5194/acp-2021-228
Preprint. Discussion started: 22 April 2021

Atmospheric Chemistry and Physics Discussions

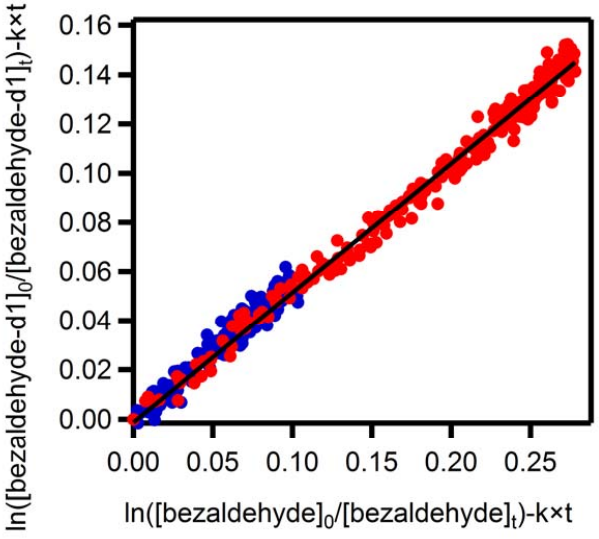

Figure 4. Ratio of initial benzaldehyde-D1 to those at other reaction times relative to those for benzaldehyde while competing for the same pool of NO_3 radicals as 0.53±0.01. The red and blue circles present two experiments with different concentrations of NO_3 radicals.

3.2.2 Reaction pathway

Linear free energy relationships comparing the reactivities of OH and NO_3 with a series of organic compounds is shown in the SI (Figure S9). Such correlations have been demonstrated in the past by Clifford et al.,(2005). We have added our measured values of k_1-k_7 to the plot. This plot suggests that the linear free energy relationship is consistent with NO_3 radicals adding to the seven aromatic aldehydes studied here. The reaction of OH radicals with aliphatic aldehydes is known to proceed through the formation of a pre-reaction complex, making the results obtained for NO_3 radicals consistent with an addition, albeit a weak adduct, pathway.

Figure 5 shows the rate coefficients for the reaction of the NO_3 radical with the seven aldehydes studied here, along with those with benzene and toluene ($<3\times10^{-17}$ and $<6.6\times10^{-17}$ cm^3 $molecule^{-1}$ s^{-1}) (Calvert et al., 2011). Benzene and toluene do not react with NO_3 to measurable extents. This observation suggests that NO_3 does not react with the aromatic ring to form a stable product. Since it is not sufficiently reactive to abstract an H atom from either the ring or the methyl group, the rate coefficient is very slow, if not zero. Therefore, the observed reaction rate coefficients suggest that the reaction proceeds via an H-atom abstraction from –CHO group (Clifford et al., 2005;Wayne et al., 1991). The rate coefficient for the reaction of NO_3 with benzaldehyde, $(2.6\pm0.3)\times10^{-15}$ cm^3 $molecule^{-1}$ s^{-1}, is similar to that with acetaldehyde $(2.7\pm0.5)\times10^{-15}$ cm^3 $molecule^{-1}$ s^{-1}, as shown in Figure 5. The mechanism for the

https://doi.org/10.5194/acp-2021-228
Preprint. Discussion started: 22 April 2021

Atmospheric Chemistry and Physics Discussions

reaction of NO_3 with acetaldehyde is believed to be H-atom abstraction from the –CHO group after the formation of a pre-reaction complex.

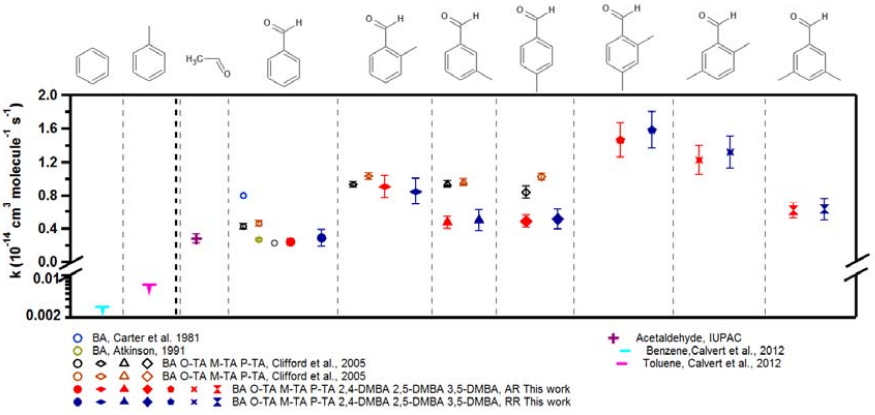

Figure 5 The measured rate coefficients for the reactions of NO_3 radical with the seven aldehydes studied here. The results of previously reported rate coefficients are also shown. The rate coefficients for acetaldehyde of $k_{(CH3CHO)}=(2.7\pm0.5)\times10^{-15}$ cm^3 molecule^{-1} s^{-1} is from IUPAC recommendations. The rate coefficients for benzene, $k_{(benzene)}<3\times10^{-17}$ cm^3 molecule^{-1} s^{-1}, and for toluene, $k_{(toluene)}\leq6.6\times10^{-17}$ cm^3 molecule^{-1} s^{-1} are from Calvert et al., 2011.

As shown in Figure 5, this work finds a higher rate coefficient for the reactions of NO_3 with ortho/meta/para-tolualdehydes than that with benzaldehyde. This enhanced reactivity with ring substitution by electron-donating groups suggests an electrophilic role for NO_3 in the reaction. Clifford et al. (2005) noted that the direct influence of the electron-donation to the ring by the CH_3 group is effectively canceled out by the electron-withdrawing effect of the –CHO group as an explanation for their measured rate coefficients being the same for all the tolualdehydes. The trends we observe for substitution of methyl groups in the tolualdehydes and the demethylated aldehydes would be consistent with electrophilic addition. Of course, the initial addition has to lead to the abstraction of the aldehydic H atom, as shown by the products and the kinetic isotope effect. Alternatively, the reactivity trend could simply be due to the C-H bond energy changes in the aldehydic group upon methyl substitution.

The C-H bond dissociation enthalpies (BDEs) of benzaldehyde and the three tolualdehydes have been obtained from Active Thermochemical Tables (ATcT). As opposed to traditional sequential thermochemistry, ATcT obtains enthalpies of formation by constructing, statistically analyzing, and solving a global thermochemical network (TN), which is formed by including experimental and theoretical determinations pertinent to the chemical species that are included in the network, as explained in more details elsewhere (Ruscic et al., 2004;Ruscic et al., 2005).

https://doi.org/10.5194/acp-2021-228
Preprint. Discussion started: 22 April 2021


Atmospheric Chemistry and Physics Discussions

The results presented here are based on the most current ATcT TN (ver. 1.122x), obtained by further expanding prior (Bross et al., 2019;Zaleski et al., 2021) versions (1.122r and 1.122v) by including species of interest to the present study, as well as other ongoing studies. The current TN incorporates ~2,350 species, interconnected by ~29,000 experimental and theoretical determinations.

Typically, the insertion of a new chemical species in the TN begins by linking the new species to the already existing species via a provisional skeleton of theoretical isodesmic reactions computed using a standard set of mid-level composite calculations carried in-house, and currently consisting of W1 (Martin and de Oliveira, 1999;Parthiban and Martin, 2001), CBS-APNO (Ochterski et al., 1996), G4 (Curtiss et al., 2007), G3X (Curtiss et al., 2000), and CBS-QB3 (Montgomery et al., 1999, 2000). This is subsequently complemented by experimental and theoretical determinations from the literature, and, when possible, by additional state-of-the-art high-level composite calculations that can deliver sub-kJ mol^{-1} accuracies. As the number and accuracy of additional determinations grows, the dependence of the final result on the determinations spanning the initial skeleton diminishes and ultimately vanishes.

However, while the enthalpies of formation of gas-phase benzaldehyde and the three tolualdehydes are linked in the TN to their condensed phases, for which there are some thermochemically-relevant experimental data in the literature, the reported BDEs rely heavily on the results of mid-level composite methods, given the paucity of literature on experimental or theoretical data involving the benzoyl and toluyl radicals and the prohibitively high cost of state-of-the-art high-level composite calculations for this size of species. Analogously, our attempts to expand the TN with dimethyl benzaldehydes and their related radicals were frustrated by virtual absence of experimental and worthwhile theoretical data in the literature, combined with the high cost of theoretical calculations even using mid-level composite methods.

The ATcT BDEs of the aldehydic C-H in benzaldehyde and the three tolualdehydes are given at 298.15 K and at 0 K in Table S7, together with the corresponding enthalpies of formation of the parents and the related radicals. While only the 298.15 K BDEs are discussed below, the corresponding 0 K BDEs (a.k.a. D_0 values) are also given in the same table and are, as expected, approximately 6.3 kJ mol^{-1} (or ~2.5 RT) lower. The ATcT uncertainties provided in Table S7 correspond to 95% confidence intervals, following the standard in thermochemistry (Ruscic, 2014;Ruscic and Bross, 2019), and were obtained by using the full ATcT covariance matrix. Consequently, when the enthalpy of formation of the radical is highly correlated to that of the parent, as happens to be true in benzaldehyde and tolualdehydes, the uncertainty of the resulting BDE is perceptibly lower than the uncertainty that would be obtained by manually propagating the uncertainties of the individual enthalpies of formation in quadrature, since the latter summation assumes zero covariances.

The ATcT BDE of the aldehydic C-H in benzaldehyde is $BDE_{298}(C_6H_5C(O)\text{-}H)$ = 380.10 ± 0.84 kJ mol^{-1}. This is noticeably higher (by 6.77 ± 0.84 kJ mol^{-1}) than the corresponding BDE of the prototypical aldehyde – acetaldehyde – for which the current version of the ATcT TN

https://doi.org/10.5194/acp-2021-228
Preprint. Discussion started: 22 April 2021

Atmospheric Chemistry and Physics Discussions

produces $BDE_{298}(CH_3C(O)\text{-}H)$ = 373.37 ± 0.29 kJ mol^{-1} (essentially unchanged from the web-accessible value in the earlier ATcT TN ver. 1.122p (Ruscic and Bross, 2020)).

Of particular relevance here is the fact that the aldehydic C-H BDEs in meta- and para-tolualdehyde, $BDE_{298}(m\text{-}CH_3C_6H_4C(O)\text{-}H)$ = 379.93 ± 1.13 kJ mol^{-1} and $BDE_{298}(p\text{-}CH_3C_6H_4C(O)\text{-}H)$ = 379.85 ± 1.13 kJ mol^{-1}, are indistinguishable (within the uncertainty) from each other and when compared to the BDE in benzaldehyde. However, in ortho-tolualdehyde, the corresponding BDE is consistently lower essentially by 4.2 kJ mol^{-1}, $BDE_{298}(o\text{-}CH_3C_6H_4C(O)\text{-}H)$ = 376.09 ± 1.13 kJ mol^{-1}, lower by 3.85 ± 1.00 kJ mol^{-1} than that of meta-tolualdehyde, 3.76 ± 1.00 kJ mol^{-1} than that in para-tolualdehyde, and 4.01 ± 0.92 kJ mol^{-1} than that in benzaldehyde. Therefore, the likely origin of the reactivity differences is simply due to the bond enthalpies in the abstraction of aldehydic H atoms.

Based on the discussion above, it appears that the preponderance of evidence is consistent with the abstraction of the aldehydic H atom. However, could such an abstraction reaction start via the addition of NO_3 to the ring followed by abstraction? To examine this possibility, we carried out quantum mechanical calculations of the reaction pathways in Reaction (1). Stationary points on the potential energy surface (PES) were optimized with the BH&HLYP density functional and 6-311G(d,p) basis set in Gaussian 16 (Becke, 1993;Frisch et al., 2016), with the exception of the NO_3 radical, for which the MP2-D3h geometry was used. This level of theory and empirical treatment of NO_3 follows Boyd's computational studies with smaller aldehydes, XCHO (X = H, F, Cl, Me) (Mora-Diez and Boyd, 2002). Single point energies were evaluated at the DLPNO-CCSD(T)/cc-pVTZ level of theory with tight SCF convergence and TightPNO cutoffs in Orca (Neese, 2012;Riplinger and Neese, 2013;Riplinger et al., 2013). Relative energetics with this basis set are essentially converged, since the effect of using cc-pVQZ on the activation barrier is less than 1 kJ mol^{-1}. The calculated PES is shown in Figure 6. Computed enthalpic and Gibbs energy changes include unscaled vibrational zero-point energies and translational, rotational and vibrational contributions at 298.15 K (Luchini et al., 2020).

https://doi.org/10.5194/acp-2021-228
Preprint. Discussion started: 22 April 2021

Atmospheric Chemistry and Physics Discussions

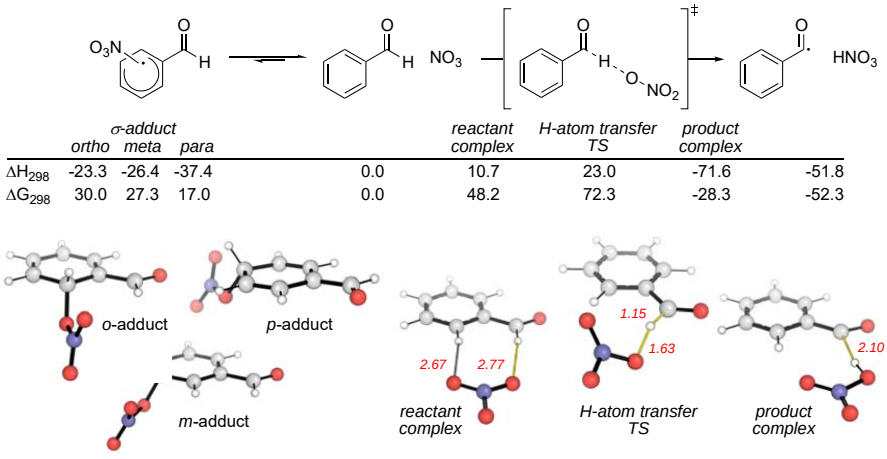

Figure 6. Pathways for reaction between BA and NO_3 calculated using DLPNO-CCSD(T)/cc-pVTZ//BH&HLYP/6-311G(d,p). Enthalpic and Gibbs energy values are in kJ/mol. Key distances in Å.

The computed reaction pathways show that the NO_3 radical is able to form a dearomatized σ-adduct (Figure 6, LHS). The most stable of these adducts (by more than 10 kJ mol^{-1}) occurs at the *para*-position. While this complexation is exothermic, due to unfavorable entropic effects it is endergonic by 17.0 kJ mol^{-1} implying this is a readily reversible process. H-atom transfer first forms a pre-reaction complex with the aldehydic group. This complex can undergo H-atom abstraction to yield the stable products observed in our experiments. Application of the Bigeleisen-Meyer equation to this H-atom transfer transition structure (TS) results in a computationally predicted primary KIE of 2.16 (2.17 with Bell's 1D-tunneling correction) (Bigeleisen and Mayer, 1947;Paton, 2016;Rzepa, 2015). This value is almost identical to the measure KIE of 1.92.

Based on this evidence, we suggest that the reactions of NO_3 with aromatic aldehydes lead to the abstraction of the aldehydic H-atom. The cleavage of the aldehydic C-H bond in this step, is consistent with the observation that a weaker BDE value is correlated with a larger reaction rate of Reaction (1). CBS-QB3 calculations (SI) imply 2,4-DMBA and 2,5-DMBA, like O-TA, have weaker aldehydic C-H bonds than the other aromatic aldehydes that lack an ortho-substituent. Since the geometry of the formyl radical is more linear than the aldehyde (the C-C-O angle increases by around 4° upon H-atom abstraction), steric strain relief is likely a contributing factor to the C-H bond weakening by an ortho-methyl substituent. Additionally, charge transfer of 0.22e from BA to NO_3 occurs in the computed H-atom transfer TS, consistent with the observation that additional electron-donating substituents, such as methyl groups), promote Reaction (1).

https://doi.org/10.5194/acp-2021-228
Preprint. Discussion started: 22 April 2021


Atmospheric Chemistry and Physics Discussions

There are potential future experiments that could shed light on the proposed reaction pathway. They include: (1) measurement of the temperature dependence of the reaction rate coefficient; (2) investigating the influence of various isotopic substitutions (e.g., OD reaction studies); (3) studying further substitution of the aromatic ring, for example with fluorine; and (4) directly detecting the radical formed in the reaction. Further quantum calculations may also be useful.

4. Atmospheric Implications

Once emitted from biomass burning and from incomplete burning of fuel to the atmosphere, the studied aromatic aldehydes could be removed through their reactions with reactive species such as OH, NO_3, and chlorine atoms. The atmospheric lifetimes of the aromatic aldehydes studied in this work have been calculated with respect to the NO_3 radical reactions using the rate coefficients, k_{aro}, obtained from this work at ambient temperature and pressure, in combination with estimated ambient tropospheric NO_3 concentrations, $[NO_3]= 5 \times 10^8$ molecules cm^{-3},(Atkinson, 1991) following the equation: $\tau_{NO3} = 1/(k_{VOC} \times [NO_3])$. We note that the NO_3 radical concentration is highly variable as noted by Brown and Stutz (Brown and Stutz, 2012), and we use this value to illustrate the relative loss rates. The calculated lifetimes are shown in Table 2. Based on our measurements, we expect that the aromatic aldehydes' atmospheric lifetimes with respect to NO_3 are 35-280 hours (for the assumed NO_3 concentrations). Table 2 also presents the lifetime of these seven aromatic aldehydes with respect to OH radicals (Spivakovsky et al., 2000) of 1×10^6 molecules cm^{-3} (again a rough value characteristic of the mid-tropospheric tropical regions) and Cl atoms (Wingenter et al., 1996) of 1×10^4 atoms cm^{-3}, and the rate coefficients taken from Calvert et al. (2011). It is clear that OH radicals contribute more than NO_3 and Cl atoms for the oxidation of the aromatic aldehyde in the atmosphere, with NO_3 reactions contributing significantly to its removal at night in the polluted area with high NOx.

https://doi.org/10.5194/acp-2021-228
Preprint. Discussion started: 22 April 2021

Atmospheric Chemistry and Physics Discussions

Table 2. Summary of rate constants and estimated atmospheric lifetimes of benzaldehyde (BA), o-tolualdehyde (O-TA), m-tolualdehyde (M-TA), p-tolualdehyde (P-TA), 2,4-dimethylbenzaldehyde (2,4-DMBA), 2,5-dimethylbenzaldehyde (2,5-DMBA) and 3,5-dimethylbenzaldehyde (3,5-DMBA) with respect to their reactions with OH, NO_3, and Cl at 298 ± 2 K and atmospheric pressure [a]

	Rate coefficients (cm^3 $molecule^{-1}$ s^{-1})			Lifetime (hours)		
	k_{OH}[b]	k_{NO3}[c]	k_{Cl}[b]	τ_{OH}	τ_{NO3}	τ_{Cl}
BA	1.26×10^{-11}	2.6×10^{-15}	9.90×10^{-11}	22	278	281
O-TA	1.89×10^{-11}	8.8×10^{-15}	1.86×10^{-10}	15	62	149
M-TA	1.68×10^{-11}	4.8×10^{-15}	1.71×10^{-10}	17	111	162
P-TA	1.68×10^{-11}	4.9×10^{-15}	1.41×10^{-10}	17	111	197
2,4-DMBA	3.12×10^{-11}	1.51×10^{-14}	8.70×10^{-11}	9	35	319
2,5-DMBA	3.15×10^{-11}	1.27×10^{-14}	9.30×10^{-11}	9	43	299
3,5-DMBA	2.78×10^{-11}	6.2×10^{-15}	9.30×10^{-11}	10	79	299

[a] Assuming [OH] = 1×10^6 molecules cm^{-3} (Spivakovsky et al., 2000) , [NO_3]=5×10^8 molecules cm^{-3} (Atkinson et al., 1991), and [Cl] = 1×10^4 (Wingenter et al., 1996). [b] the rate coefficients were extracted from Calvert et al. (2011). [c] recommended values in Table S5.

This work also found that the aromatic PAN-type compounds, for example, was the main product formed from the reaction of aromatic aldehydes with NO_3 radical. Formation of such compounds enables the transport and release of NOx to the remote troposphere, leading to the production of O_3. Such a situation may occur in wildland fire plumes.

Data availability

The compiled datasets used to produce each figure within this paper are available as Igor Pro files upon request.

Supplement

The supplement related to this article is available online at:

Author contributions

YR and ARR wrote the paper with input from all authors. YR and LZ conducted the experiments and analyzed the data, MM helped with the analysis of the data. MI, VD and SSB were responsible for the CRDS instrument. BR and RSP made the theoretical calculations. AM and ARR designed the experiments and led the study. All coauthors commented on the paper.

Competing interests

The authors declare that they have no conflict of interest.

https://doi.org/10.5194/acp-2021-228
Preprint. Discussion started: 22 April 2021

Atmospheric Chemistry and Physics Discussions

Acknowledgements

We are grateful to Timothy Wallington for the IR cross sections of BAPAN. Work of ARR was supported by Le Studium and CSU.

Financial support. This work is supported by the European Union's Horizon 2020 research and innovation programme through the EUROCHAMP-2020 Infrastructure Activity under grant agreement No. 730997, Labex Voltaire (ANR-10-LABX-100-01), ANR (SEA_M project, ANR-16-CE01-0013, program ANR-RGC 2016) and National Natural Science Foundation of China (21976106). Work of BR was supported by the U.S. Department of Energy, Office of Science, Office of Basic Energy Sciences, Division of Chemical Sciences, Geosciences, and Biosciences through the Gas-Phase Chemical Physics Program under contract No. DE-AC02-06CH11357. RSP acknowledges the use of the RMACC Summit supercomputer, which is supported by the National Science Foundation (ACI-1532235 and ACI-1532236), the University of Colorado Boulder and Colorado State University, and the Extreme Science and Engineering Discovery Environment (XSEDE) through allocation TG-CHE180056.

https://doi.org/10.5194/acp-2021-228
Preprint. Discussion started: 22 April 2021

Atmospheric Chemistry and Physics Discussions

References

Atkinson, R., Aschmann, S. M., Winer, A. M., and Pitts, J. N.: Kinetics of the gas-phase reactions of nitrate radicals with a series of dialkenes, cycloalkenes, and monoterpenes at 295 ± 1 K, Environ. Sci. Technol., 18, 370-375, 10.1021/es00123a016, 1984.

Atkinson, R.: Kinetics and Mechanisms of the Gas‐Phase Reactions of the NO_3 Radical with Organic Compounds, Journal of Physical and Chemical Reference Data, 20, 459-507, doi:http://dx.doi.org/10.1063/1.555887, 1991.

Becke, A. D.: A new mixing of Hartree-Fock and local density-functional theories, The Journal of Chemical Physics, 98, 1372-1377, 10.1063/1.464304, 1993.

Bigeleisen, J., and Mayer, M. G.: Calculation of Equilibrium Constants for Isotopic Exchange Reactions, The Journal of Chemical Physics, 15, 261-267, 10.1063/1.1746492, 1947.

Bossmeyer, J., Brauers, T., Richter, C., Rohrer, F., Wegener, R., and Wahner, A.: Simulation chamber studies on the NO_3 chemistry of atmospheric aldehydes, Geophysical Research Letters, 33, n/a-n/a, 10.1029/2006GL026778, 2006.

Brauers, T., and Finlayson-Pitts, B. J.: Analysis of relative rate measurements, International Journal of Chemical Kinetics, 29, 665-672, 10.1002/(SICI)1097-4601(1997)29:9<665::AID-KIN3>3.0.CO;2-S, 1997.

Bross, D. H., Yu, H.-G., Harding, L. B., and Ruscic, B.: Active Thermochemical Tables: The Partition Function of Hydroxymethyl (CH_2OH) Revisited, The Journal of Physical Chemistry A, 123, 4212-4231, 10.1021/acs.jpca.9b02295, 2019.

Brown, S. S., Stark, H., Ciciora, S. J., McLaughlin, R. J., and Ravishankara, A. R.: Simultaneous in situ detection of atmospheric NO_3 and N_2O_5 via cavity ring-down spectroscopy, Review of Scientific Instruments, 73, 3291-3301, doi:http://dx.doi.org/10.1063/1.1499214, 2002.

Brown, S. S., and Stutz, J.: Nighttime radical observations and chemistry, Chemical Society Reviews, 41, 6405-6447, 10.1039/C2CS35181A, 2012.

Calvert, J. G., Atkinson, R., Becker, K. H., Kamens, R. M., Seinfeld, J. H., Wallington, T. J., and Yarwood, G.: The Mechanisms of Atmospheric Oxidation of Aromatic Hydrocarbons, Oxford University Press, London, 2002.

Calvert, J. G., Mellouki, A., Orlando, J. J., Pilling, M. J., and Wallington, T. J.: The Mechanisms of Atmospheric Oxidation of the Oxygenates, Oxford University Press, New York, 2011.

Caralp, F., Foucher, V., Lesclaux, R., J. Wallington, T., and D. Hurley, M.: Atmospheric chemistry of benzaldehyde: UV absorption spectrum and reaction kinetics and mechanisms of the $C_6H_5C(O)O_2$ radical, Physical Chemistry Chemical Physics, 1, 3509-3517, 10.1039/A903088C, 1999.

Carter, W. P. L., Winer, A. M., and Pitts, J. N.: Major atmospheric sink for phenol and the cresols. Reaction with the nitrate radical, Environmental Science & Technology, 15, 829-831, 10.1021/es00089a009, 1981.

Clifford, G. M., Thüner, L. P., Wenger, J. C., and Shallcross, D. E.: Kinetics of the gas-phase reactions of OH and NO_3 radicals with aromatic aldehydes, Journal of Photochemistry and Photobiology A: Chemistry, 176, 172-182, http://dx.doi.org/10.1016/j.jphotochem.2005.09.022, 2005.

Curtiss, L. A., Redfern, P. C., Raghavachari, K., and Pople, J. A.: Gaussian-3X (G3X) theory: Use of improved geometries, zero-point energies, and Hartree–Fock basis sets, The Journal of Chemical Physics, 114, 108-117, 10.1063/1.1321305, 2000.

Curtiss, L. A., Redfern, P. C., and Raghavachari, K.: Gaussian-4 theory, Journal of Chemical Physics, 126, 084108, 10.1063/1.2436888, 2007.

Dubé, W. P., Brown, S. S., Osthoff, H. D., Nunley, M. R., Ciciora, S. J., Paris, M. W., McLaughlin, R. J., and Ravishankara, A. R.: Aircraft instrument for simultaneous, in situ measurement of NO_3 and N_2O_5 via pulsed cavity ring-down spectroscopy, Review of Scientific Instruments, 77, 034101, 10.1063/1.2176058, 2006.

Frisch, M. J., Trucks, G. W., Schlegel, H. B., Scuseria, G. E., Robb, M. A., Cheeseman, J. R., Scalmani, G., Barone, V., Petersson, G. A., Nakatsuji, H., Li, X., Caricato, M., Marenich, A. V., Bloino, J., Janesko, B. G., Gomperts, R., Mennucci, B., Hratchian, H. P., Ortiz, J.

https://doi.org/10.5194/acp-2021-228
Preprint. Discussion started: 22 April 2021

V., Izmaylov, A. F., Sonnenberg, J. L., Williams, Ding, F., Lipparini, F., Egidi, F., Goings, J., Peng, B., Petrone, A., Henderson, T., Ranasinghe, D., Zakrzewski, V. G., Gao, J., Rega, N., Zheng, G., Liang, W., Hada, M., Ehara, M., Toyota, K., Fukuda, R., Hasegawa, J., Ishida, M., Nakajima, T., Honda, Y., Kitao, O., Nakai, H., Vreven, T., Throssell, K., Montgomery Jr., J. A., Peralta, J. E., Ogliaro, F., Bearpark, M. J., Heyd, J. J., Brothers, E. N., Kudin, K. N., Staroverov, V. N., Keith, T. A., Kobayashi, R., Normand, J., Raghavachari, K., Rendell, A. P., Burant, J. C., Iyengar, S. S., Tomasi, J., Cossi, M., Millam, J. M., Klene, M., Adamo, C., Cammi, R., Ochterski, J. W., Martin, R. L., Morokuma, K., Farkas, O., Foresman, J. B., and Fox, D. J.: Gaussian 16 Rev. C.01, in, Wallingford, CT, 2016.

J. B. Burkholder, S. P. Sander, J. Abbatt, J. R. Barker, R. E. Huie, C. E. Kolb, M. J. Kurylo, V. L. Orkin, D. M. Wilmouth, and Wine, P. H.: Chemical Kinetics and Photochemical Data for Use in Atmospheric Studies, Evaluation No. 18, in, edited by: JPL Publication 15-10, J. P. L., Pasadena,, 2015.

Koss, A. R., Sekimoto, K., Gilman, J. B., Selimovic, V., Coggon, M. M., Zarzana, K. J., Yuan, B., Lerner, B. M., Brown, S. S., Jimenez, J. L., Krechmer, J., Roberts, J. M., Warneke, C., Yokelson, R. J., and de Gouw, J.: Non-methane organic gas emissions from biomass burning: identification, quantification, and emission factors from PTR-ToF during the FIREX 2016 laboratory experiment, Atmos. Chem. Phys., 18, 3299-3319, 10.5194/acp-18-3299-2018, 2018.

Legreid, G., Reimann, S., Steinbacher, M., Staehelin, J., Young, D., and Stemmler, K.: 'Measurements of OVOCs and NMHCs in a Swiss Highway Tunnel for Estimation of Road Transport Emissions, Environmental Science & Technology, 41, 7060-7066, 10.1021/es062309+, 2007.

Luchini, G., Alegre-Requena, J., Funes-Ardoiz, I., and Paton, R.: GoodVibes: automated thermochemistry for heterogeneous computational chemistry data [version 1; peer review: 2 approved with reservations], F1000Research, 9, 10.12688/f1000research.22758.1, 2020.

Martin, J. M. L., and de Oliveira, G.: Towards standard methods for benchmark quality ab initio thermochemistry—W1 and W2 theory, The Journal of Chemical Physics, 111, 1843-1856, 10.1063/1.479454, 1999.

Montgomery, J. A., Frisch, M. J., Ochterski, J. W., and Petersson, G. A.: A complete basis set model chemistry. VI. Use of density functional geometries and frequencies, The Journal of Chemical Physics, 110, 2822-2827, 10.1063/1.477924, 1999.

Montgomery, J. A., Frisch, M. J., Ochterski, J. W., and Petersson, G. A.: A complete basis set model chemistry. VII. Use of the minimum population localization method, The Journal of Chemical Physics, 112, 6532-6542, 10.1063/1.481224, 2000.

Mora-Diez, N., and Boyd, R. J.: A Computational Study of the Kinetics of the NO_3 Hydrogen-Abstraction Reaction from a Series of Aldehydes (XCHO: X = F, Cl, H, CH_3), The Journal of Physical Chemistry A, 106, 384-394, 10.1021/jp0125000, 2002.

Neese, F.: The ORCA program system, WIREs Computational Molecular Science, 2, 73-78, 10.1002/wcms.81, 2012.

Obermeyer, G., Aschmann, S. M., Atkinson, R., and Arey, J.: Carbonyl atmospheric reaction products of aromatic hydrocarbons in ambient air, Atmospheric Environment, 43, 3736-3744, 10.1016/j.atmosenv.2009.04.015, 2009.

Ochterski, J. W., Petersson, G. A., and Montgomery, J. A.: A complete basis set model chemistry. V. Extensions to six or more heavy atoms, The Journal of Chemical Physics, 104, 2598-2619, 10.1063/1.470985, 1996.

Organization for Economic Co-operation and Development, OECD integrated HPV database: http://cs3-hq.oecd.org/scripts/hpv/index.asp, 2002.

Parthiban, S., and Martin, J. M. L.: Assessment of W1 and W2 theories for the computation of electron affinities, ionization potentials, heats of formation, and proton affinities, The Journal of Chemical Physics, 114, 6014-6029, 10.1063/1.1356014, 2001.

Paton, R.: Kinisot: v 1.0.0 public API for Kinisot.py. Zenodo., KINISOT, Zenodo., 10.5281/zenodo.60082, 2016.

Platz, J., Nielsen, O. J., Wallington, T. J., Ball, J. C., Hurley, M. D., Straccia, A. M., Schneider,

https://doi.org/10.5194/acp-2021-228
Preprint. Discussion started: 22 April 2021

W. F., and Sehested, J.: Atmospheric Chemistry of the Phenoxy Radical, $C_6H_5O(\bullet)$: UV Spectrum and Kinetics of Its Reaction with NO, NO_2, and O_2, The Journal of Physical Chemistry A, 102, 7964-7974, 10.1021/jp9822211, 1998.

Riplinger, C., and Neese, F.: An efficient and near linear scaling pair natural orbital based local coupled cluster method, The Journal of Chemical Physics, 138, 034106, 10.1063/1.4773581, 2013.

Riplinger, C., Sandhoefer, B., Hansen, A., and Neese, F.: Natural triple excitations in local coupled cluster calculations with pair natural orbitals, The Journal of Chemical Physics, 139, 134101, 10.1063/1.4821834, 2013.

Ruscic, B., Pinzon, R. E., Morton, M. L., von Laszevski, G., Bittner, S. J., Nijsure, S. G., Amin, K. A., Minkoff, M., and Wagner, A. F.: Introduction to Active Thermochemical Tables: Several "Key" Enthalpies of Formation Revisited, The Journal of Physical Chemistry A, 108, 9979-9997, 10.1021/jp047912y, 2004.

Ruscic, B., Pinzon, R. E., Laszewski, G. v., Kodeboyina, D., Burcat, A., Leahy, D., Montoya, D., and Wagner, A. F.: Active Thermochemical Tables: thermochemistry for the 21st century, Journal of Physics: Conference Series, 16, 561-570, 10.1088/1742-6596/16/1/078, 2005.

Ruscic, B.: Uncertainty quantification in thermochemistry, benchmarking electronic structure computations, and Active Thermochemical Tables, International Journal of Quantum Chemistry, 114, 1097-1101, 10.1002/qua.24605, 2014.

Ruscic, B., and Bross, D. H.: Thermochemistry, Computer Aided Chemical Engineering, 45, 3-114, 10.1016/B978-0-444-64087-1.00001-2, 2019.

Ruscic, B., and Bross, D. H.: Active Thermochemical Tables (ATcT) values based on ver. 1.122p of the Thermochemical Network; available at ATcT.anl.gov, 2020.

Rzepa, H. S.: KINISOT. A basic program to calculate kinetic isotope effects using normal coordinate analysis of transition state and reactants., KINISOT, Zenodo., 10.5281/zenodo.19272, 2015.

Spivakovsky, C. M., Logan, J. A., Montzka, S. A., Balkanski, Y. J., Foreman-Fowler, M., Jones, D. B. A., Horowitz, L. W., Fusco, A. C., Brenninkmeijer, C. A. M., Prather, M. J., Wofsy, S. C., and McElroy, M. B.: Three-dimensional climatological distribution of tropospheric OH: Update and evaluation, Journal of Geophysical Research: Atmospheres, 105, 8931-8980, 10.1029/1999JD901006, 2000.

Wayne, R. P., Barnes, I., Biggs, P., Burrows, J. P., Canosamas, C. E., Hjorth, J., Lebras, G., Moortgat, G. K., Perner, D., Poulet, G., Restelli, G., and Sidebottom, H.: The nitrate radical - Physics, Chemistry, and the Atmosphere, Atmospheric Environment Part a-General Topics, 25, 1-203, 10.1016/0960-1686(91)90192-a, 1991.

Wayne, R. P.: Chemistry of Atmospheres: An Introduction to the Chemistry of the Atmospheres of Earth, the Planets, and their Satellites, 3 (28 December 2000) ed., Oxford University Press, Oxford, 2000.

Wingenter, O. W., Kubo, M. K., Blake, N. J., Smith, T. W., Blake, D. R., and Rowland, F. S.: Hydrocarbon and halocarbon measurements as photochemical and dynamical indicators of atmospheric hydroxyl, atomic chlorine, and vertical mixing obtained during Lagrangian flights, Journal of Geophysical Research: Atmospheres, 101, 4331-4340, 10.1029/95JD02457, 1996.

Zaleski, D. P., Sivaramakrishnan, R., Weller, H. R., Seifert, N. A., Bross, D. H., Ruscic, B., Moore III, K. B., Elliott, S. N., Copan, A. V., Harding, L. B., Klippenstein, S. J., Field, R. W., and Prozument, K.: Substitution reactions in the pyrolysis of acetone revealed through a modeling, experiment, theory (MET) paradigm, Journal of the American Chemical Society, 143, 3124-3142, 10.1021/jacs.0c11677, 2021.

Zhou, L., Ravishankara, A. R., Brown, S. S., Idir, M., Zarzana, K. J., Daële, V., and Mellouki, A.: Kinetics of the Reactions of NO_3 Radical with Methacrylate Esters, The Journal of Physical Chemistry A, 121, 4464-4474, 10.1021/acs.jpca.7b02332, 2017.

Zhou, L., Ravishankara, A. R., Brown, S. S., Zarzana, K. J., Idir, M., Daële, V., and Mellouki, A.: Kinetics of the reactions of NO_3 radical with alkanes, Physical Chemistry Chemical Physics, 21, 4246-4257, 10.1039/C8CP07675H, 2019.